

# Temporal and Triggered Evolution of Host–Guest Characteristics in Amphiphilic Polymer Assemblies

Poornima Rangadurai, Mijanur Rahaman Molla, Priyaa Prasad, Matthew Caissy, and S. Thayumanavan\*

Department of Chemistry, University of Massachusetts, 710 N. Pleasant Street, Amherst, Massachusetts 01003-9336, United States

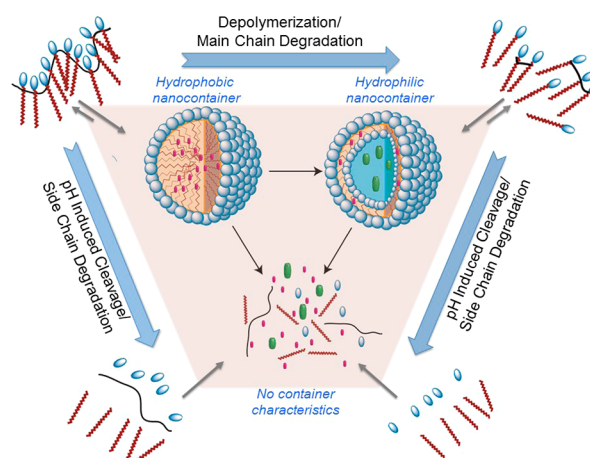
**S** Supporting Information

**ABSTRACT:** An amphiphilic polymer with cleavable side chain and main chain functional groups has been designed and synthesized. Specific cleavage of either of its functional groups was found to have an effect on the morphology of the assembly. Degradation of the main chain is shown to cause morphology of the supramolecular assembly to evolve with time from a micelle-like assembly to a vesicular assembly. On the other hand, stimulus-induced cleavage of the side chains causes these nanoassemblies to disassemble. These temporal (main chain) and triggered (side chain) degradation processes have implications in the design of degradable polymers as supramolecular scaffolds for biological applications.

Supramolecular assembly of amphiphilic molecules has been of considerable interest due to their potential utility in a variety of applications.<sup>1</sup> Over the years, research in amphiphilic assemblies has evolved from designing molecules to obtain well-defined morphologies to incorporating stimuli-sensitive characteristics in these assemblies to develop them as smart nanomaterials.<sup>2</sup> Polymeric amphiphiles have garnered attention due to the enhanced kinetic and thermodynamic stabilities of the nanoassemblies. Block copolymers have gained particular attention here, because of the conveniently derivable structure–property correlations in terms of the two blocks.<sup>3</sup> On the other hand, the possibility of preprogramming self-assembly characteristics in the monomer stage itself has attracted interest in amphiphilic homopolymer systems.<sup>4</sup> Since these amphiphiles are simply the polymerized versions of the corresponding small molecules, there exists a structural continuum between these two molecular classes in the form of oligomers. In this context, we study the host–guest characteristics and morphological evolution of assemblies made from low molecular weight polymeric amphiphiles in response to their depolymerization toward monomeric amphiphile (Scheme 1). We disclose our preliminary findings here.

For this study, we designed a short amphiphilic polymer that has two disparate degradable features. First, the polymer has been designed such that the depolymerization process is slow to allow for the evaluation of morphological changes. Complementary to the depolymerization event, the second mechanism involves a triggered change in the amphiphilicity of the polymer to potentially cause complete disassembly. We use both these processes to interrogate the system over time. Polyurethanes, containing  $\beta$ -thioester linkages, have been designed to satisfy these requirements. The carbamate linkers

**Scheme 1. Schematic of Host–Guest Characteristic Evolutions in Response to Main- or Side- Chain Degradation of Amphiphilic Polymer**



in the polyurethane backbone are known to hydrolytically degrade slowly in aqueous phase,<sup>5</sup> and thus it satisfies the first requirement. Most of the reported amphiphilic polyurethanes are based on difference in the hydrophilicities of the comonomers in the backbone.<sup>6</sup> The design requirements here however dictate that the monomer building block itself be amphiphilic so that the degradation of the polymer would lead to shorter oligomers with the overall amphiphilicity retained in the system (Scheme 1). Moreover, the polymer and the monomer should also fulfill the triggerable disassembly requirement mentioned above. The targeted monomer containing  $\beta$ -thioester moieties provides this opportunity, as these have been shown to undergo faster hydrolysis at lower pH.<sup>7</sup>

The molecular design that could satisfy all these design requirements is shown as polymer **P1** (Figure 1a). The polyurethane **P1** constitutes an amphiphilic monomer **M1** (Scheme 2), derived from dithiothreitol (DTT). The molecular weight ( $M_n$ ) of the polymer was found to be 7.5 kDa and quite polydisperse. The short polymer provides an ideal scaffold for observing morphological evolutions upon subtle changes in the structure. Synthetic and characterization details are provided in the Supporting Information (SI).

To study the amphiphilicity-based self-assembly of **P1**, the polymer was dispersed in water at different concentrations in

Received: April 21, 2016

Published: June 3, 2016

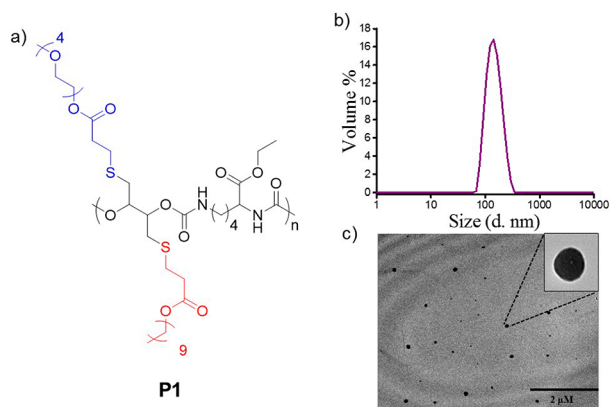
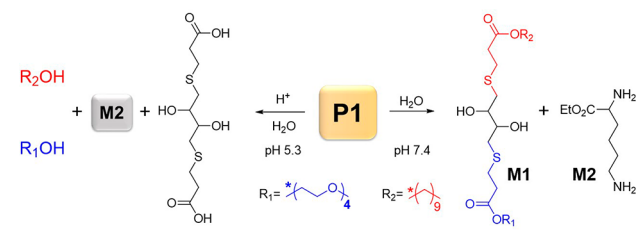


**Figure 1.** (a) Structure of **P1**. (b) DLS of aqueous solution of **P1**. (c) TEM image indicating micellar aggregates (Inset: micelle-like assembly of same size captured at higher magnification).

### Scheme 2. Products of $\beta$ -Thioester and Urethane Hydrolysis at pH 5.3 and 7.4, Respectively



the presence of a spectroscopic probe, Nile red (NR). NR is insoluble in aqueous phase by itself, but is apparently soluble in the presence of **P1**. This suggests that the polymer is capable of providing hydrophobic pockets for guest encapsulation. To investigate whether this solubilization is due to aggregation of the polymer to form a hydrophobic pocket, NR fluorescence was monitored at different concentrations of the polymer. The sharp increase in the fluorescence at a specific concentration indicates the onset of the polymer aggregation at  $\sim 0.06$  mg/mL, which is considered to be the critical aggregate concentration (CAC) of **P1** (see SI). To investigate the size and morphology of such an assembly, the polymer was studied by dynamic light scattering (DLS) (Figure 1b) and transmission electron microscopy (TEM) (Figure 1c). TEM images show that the observed aggregates are spherical with a solid core, with a size of a little over 100 nm. Considering the hydrophobicity of the interior from the guest encapsulation study, these aggregates were considered to be complex micelle-like aggregates, which has been typical of amphiphilic homopolymer assemblies.<sup>8</sup> TEM images are obtained from dry samples, whereas the system is being studied in solution. The close correlation in the sizes of the aggregates obtained from TEM and those from DLS in solution ( $\sim 130$  nm, Figure 1b), along with the dye incorporation studies, suggests that **P1** indeed exhibits these micelle-like assemblies in aqueous phase.

Since the polymer **P1** was designed to be sensitive to change in pH, change in the container property of the amphiphilic assembly at lower pH was evaluated. Release of the encapsulated NR in 0.1 mg/mL **P1** in pH 5.3 TRIS buffer was monitored over several hours. Dye release started soon after the pH buffer was lowered, resulting in 32% release in the first 10 h and ultimately reaching  $\sim 95\%$  release in 6 days. This can be attributed to the hydrolysis of  $\beta$ -thioester bonds at pH

5.3, disrupting the amphiphilic character of the polymer and its propensity to form the nanoassembly. The control study at pH 7.4, where  $<15\%$  dye release in 7 days, supports the hypothesis that the guest release is due to the pH-induced disruption of  $\beta$ -thioesters (Figure 2a–c).

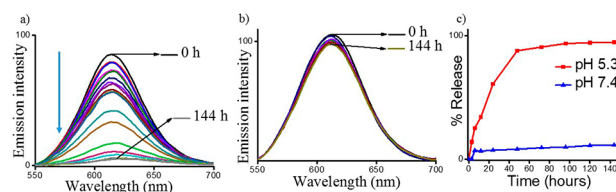


**Figure 2.** Time-dependent fluorescence emission of Nile red encapsulated **P1** treated to (a) pH 5 and (b) pH 7.4. (c) % Release of Nile red at pH 5.3 and 7.4 from **P1** micelles, plotted against time.

An interesting observation was made when a further validation of the observed guest molecule release was attempted using DLS. Although the assemblies disappeared as anticipated at pH 5.3, the result from the control experiment at pH 7.4 was surprising. At pH 5.3, the 130 nm assembly disappeared over time to afford micron-sized aggregates (Figure 3a), which are

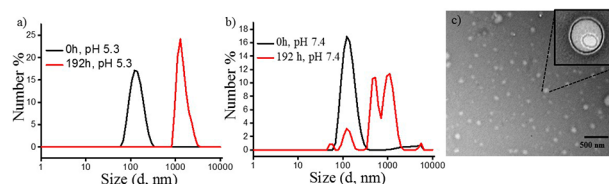


**Figure 3.** DLS plots of **P1** before and after (a) treatment to acidic pH 5.3 and (b) treatment with tris buffer pH 7.4. (c) TEM images of **P1**, after 8 days at pH 7.4, revealing vesicles of various sizes (Inset: vesicles of same size captured at higher magnification).

attributed to the hydrophobic byproducts of the pH-induced cleavage (Scheme 2). Interestingly, the control solution at pH 7.4 showed a variety of size distributions after day 7, including at 50 and 100 nm in addition to some larger aggregates (Figure 3b). The presence of smaller assemblies was especially baffling. To further investigate this, the aged samples were analyzed by TEM, which indicated the presence of vesicular aggregates with an aqueous lumen (Figure 3c). Sizes of these assemblies were mostly between 40 and 100 nm, though some larger ( $\sim 500$  nm) vesicles were also observed (Figure 3c). Considering the sample at pH 5.3 did not exhibit similar changes, we hypothesized that the urethane backbone has hydrolyzed slowly over 8 days, forming smaller oligomers, which prefer the formation of vesicles. Note that the urethane hydrolysis retains the amphiphilicity in the resultant oligomers, while the hydrolysis of  $\beta$ -thioester moiety disrupts it (Scheme 2). To test this possibility, we characterized the assemblies formed by the monomer **M1**, as this represents the final product of the degradation of carbamate moieties in the polyurethane backbone. Indeed, the morphology of the assembly formed by **M1** was found to be vesicular with  $\sim 100$  nm size (Figure 4a), similar to those observed with **P1** after 7 days.

To further test the hypothesis of depolymerization-induced morphological change, we tested the molecular weight evolution of the polymer by lyophilizing the sample on days 1, 4, and 8 and by testing them in GPC. If our degradation hypothesis is correct, we would see new peaks corresponding to

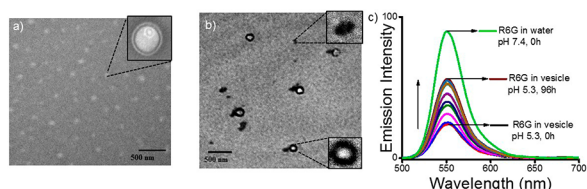


**Figure 4.** TEM images of (a) **M1** indicating vesicles (Inset: vesicles of same size captured at higher magnification) and (b) **P1** on day 4 sample revealing both micelles and vesicles (Inset: zoomed-in to show the morphological mixtures). (c) R6G release from aged **P1** vesicles at pH 5.3.

oligomers and a longer retention time (see SI). Indeed, the GPC showed new peaks at longer retention times over the course of 8 days, the molecular weights of which correspond to tetramers, trimers, and dimers. Observable extent of shorter oligomer formation was found from day 4, and the peak corresponding to **P1** disappeared completely by day 8. Next, we investigated whether this depolymerization-induced change occurred via any intermediate morphologies. On day 4, the GPC peaks for polymer **P1** and shorter oligomers were concurrently observed. TEM images of this sample showed a distinct mixture of vesicles and micelles (Figure 4b).

Finally, we were interested in investigating this depolymerization-induced morphological change using the host–guest characteristics differences between micellar and vesicular aggregates. While both these assemblies would be able to sequester hydrophobic guests, because of the hydrophobicity of the micellar interior and the vesicular membranes, only the latter would be able to sequester hydrophilic guests. Indeed, we were unsuccessful in our attempts to incorporate hydrophilic rhodamine 6G (R6G) within the polymer assembly **P1**. Interestingly, however, R6G was comfortably incorporated within the vesicular assembly formed by **M1**, which was ascertained by comparing the absorbance-matched solutions of R6G in water (see SI). The observed fluorescence self-quenching, due to local concentration effects imposed by encapsulation, suggests that the hydrophilic dye has been incorporated within the lumen of the vesicular assemblies. If **P1** indeed depolymerizes to smaller oligomers, which have the propensity to form vesicular assemblies, the ability to sequester hydrophilic molecules must evolve with time. Indeed, we found that the hydrophilic dye can be encapsulated in aged **P1** on day 8. Note that our hypothesis here is that the urethane bond hydrolyzes, but the  $\beta$ -thioester bonds are intact during the aging process. If this was correct, then lowering the pH of the solution containing the assembly based on monomer **M1** or the aged **P1** should cause disassembly, because the amphiphilic character of the constituent molecules would disappear due to the pH-induced hydrolysis of the  $\beta$ -thioester. The observed decrease in self-quenching of R6G with time at pH 5.3 in both these solutions (Figure 4c and SI) supports this hypothesis.

In summary, by designing an amphiphilic homopolymer that can degrade both at the side and the main chains, we have shown that the morphology of the assembly and its host–guest characteristics can be predictably evolved. The amphiphilic polymer itself forms a micelle-like assembly in aqueous phase, where it is capable of acting as a nanocontainer for hydrophobic guest molecules. Subjecting this assembly to a pH change causes it to lose this container property, because of the degradation of the side chain functionalities. On the other hand, aging this assembly in aqueous solution results in slow

depolymerization through degradation of the main chain, where the morphology of the assembly changes from micelle-like structures to vesicular ones. This morphological change accompanies an evolution in host–guest characteristics, where the assembly changes from a nanocontainer for hydrophobic guest molecules to one that can be a concurrent container for both hydrophobic and hydrophilic guest molecules. Lowering the solution pH causes the assembly to lose its ability to encapsulate both types of guest molecules. The evolution of these assemblies in response to depolymerization might be reminiscent of the polymerization-induced self-assembly process,<sup>9</sup> which has recently gained much attention. Note however that the process is sharply distinct, because the hydrophilic–lipophilic balance in the amphiphilic polymer does not evolve with the depolymerization process noted here. Therefore, the morphological changes observed here are dictated by the molecular architecture rather than by the relative volumes of the amphiphilic constituents. The variations in the molecular architecture between these oligomers and the monomer likely arise from the fact that the amphiphilic building blocks in the oligomers are more conformationally restricted with respect to each other, compared to the monomers. The observations here raise several interesting questions. From a fundamental perspective, it is interesting to ask whether the mixture of two morphologies after 4 days is an indicator of self-selection among oligomeric amphiphiles, driven by their preferred morphologies. Addressing these questions, along with exploring the potential utility of these assemblies in meaningful applications, will be part of our future efforts in this area. From an applications perspective, degradable amphiphiles have drawn significant attention due to their potential use in biological applications such as delivery and diagnostics. The fact that both polymer and monomer were found to be non-cytotoxic to cells (see SI) suggests the potential for utilizing these assemblies in such applications.

## ■ ASSOCIATED CONTENT

### 📄 Supporting Information

The Supporting Information is available free of charge on the ACS Publications website at DOI: 10.1021/jacs.6b04099.

Materials and methods, experimental details/results, and characterization data (NMR, GPC, TEM) (PDF)

## ■ AUTHOR INFORMATION

### Corresponding Author

\*thai@chem.umass.edu

### Notes

The authors declare no competing financial interest.

## ■ ACKNOWLEDGMENTS

We are grateful to partial support from the NSF (CHE-1307118) and the NIH (GM-065255). We thank Dr. Rinat Abzalimov and Bo Zhao for their help with mass spectra.

## ■ REFERENCES

- (1) (a) Whitesides, G. M.; Mathias, J. P.; Seto, C. T. *Science* **1991**, 254, 1312. (b) Aida, T.; Meijer, E. W.; Stupp, S. I. *Science* **2012**, 335, 813. (c) Tu, R. S.; Tirrell, M. *Adv. Drug Delivery Rev.* **2004**, 56, 1537. (d) Tantakitti, F.; Boekhoven, J. B.; Wang, X.; Kazantsev, R. V.; Yu, T.; Li, J.; Zhuang, E.; Zandi, R.; Ortony, J. H.; Newcomb, C. J.; Palmer, L. C.; Shekhawat, G. S.; de la Cruz, M. O.; Schatz, G. C.; Stupp, S. I. *Nat.*

*Mater.* **2016**, *15*, 469. (e) Soussan, E.; Cassel, S.; Blanzat, M.; Rico-Lattes, I. *Angew. Chem., Int. Ed.* **2009**, *48*, 274.

(2) (a) Angelova, A.; Angelov, B.; Mutafchieva, R.; Lesieur, S.; Couvreur, P. *Acc. Chem. Res.* **2011**, *44*, 147. (b) Theato, P.; Sumerlin, B. S.; O'Reilly, R. K.; Epps, T. H., III *Chem. Soc. Rev.* **2013**, *42*, 7055.

(3) (a) Mai, Y.; Eisenberg, A. *Chem. Soc. Rev.* **2012**, *41*, 5969. (b) Hu, H.; Gopinadhan, M.; Osuji, C. O. *Soft Matter* **2014**, *10*, 3867.

(4) Kale, T.; Klaikherd, A.; Popere, B.; Thayumanavan, S. *Langmuir* **2009**, *25*, 9660.

(5) Mondal, S.; Martin, D. *Polym. Degrad. Stab.* **2012**, *97*, 1553.

(6) For examples, see: (a) Cherng, J. Y.; Hou, T. Y.; Shih, M. F.; Talsma, H.; Hennink, W. E. *Int. J. Pharm.* **2013**, *450*, 145. (b) Tseng, S. J.; Tang, S. C. *Biomacromolecules* **2007**, *8*, 50. (c) Pan, Z.; Yu, L.; Song, N.; Zhou, L.; Li, J.; Ding, M.; Tan, H.; Fu, Q. *Polym. Chem.* **2014**, *5*, 2901. (d) Ma, N.; Li, Y.; Xu, H.; Wang, Z.; Zhang, X. *J. Am. Chem. Soc.* **2010**, *132*, 442. (e) Yang, T.; Chin, W.; Cherng, J.; Shau, M. *Biomacromolecules* **2004**, *5*, 1926.

(7) (a) Dan, K.; Ghosh, S. *Angew. Chem., Int. Ed.* **2013**, *52*, 7300. (b) Schoenmakers, R. G.; Van de Wetering, P.; Elbert, D. L.; Hubbell, J. A. *J. Controlled Release* **2004**, *95*, 291.

(8) (a) Savariar, E. N.; Aathimanikandan, S. V.; Thayumanavan, S. *J. Am. Chem. Soc.* **2006**, *128*, 16224. (b) Basu, S.; Vutukuri, D.; Thayumanavan, S. *J. Am. Chem. Soc.* **2005**, *127*, 16794.

(9) Warren, N. J.; Armes, S. P. *J. Am. Chem. Soc.* **2014**, *136*, 10174.